

# Calculation of a Deuterium Double Shock Hugoniot from *Ab initio* Simulations

B. Militzer

*Lawrence Livermore National Laboratory, University of California, Livermore, CA 94550*

D. M. Ceperley

*Department of Physics, National Center for Supercomputing Applications,  
University of Illinois at Urbana-Champaign, Urbana, IL 61801*

J. D. Kress, J. D. Johnson, L. A. Collins, and S. Mazevet

*Theoretical Division, Los Alamos National Laboratory, Los Alamos, New Mexico 87545*

(Dated: November 1, 2018)

We calculate the equation of state of dense deuterium with two *ab initio* simulations techniques, path integral Monte Carlo and density functional theory molecular dynamics, in the density range of  $0.67 \leq \rho \leq 1.60 \text{ g cm}^{-3}$ . We derive the double shock Hugoniot and compare with the recent laser-driven double shock wave experiments by Mostovych et al. [9]. We find excellent agreement between the two types of microscopic simulations but a significant discrepancy with the laser-driven shock measurements.

Single-shock laser experiments on liquid deuterium have probed the equation of state (EOS) up to 340 GPa [1] and have measured a significantly higher compressibility than predicted by standard models like Sesame [2] and by more recent experiments using magnetic drives [3]. The laser-driven experimental findings also disagree with results from first principles simulations [4, 5, 6] and leave only some chemical models in agreement [7, 8]. The EOS is of fundamental importance to our understanding of many physical phenomena such as the Jovian planets, inertial confinement fusion, and pulsed-power produced plasmas.

In the recent laser-driven double shock (DS) experiments by Mostovych et al. [9], final pressures of 100-600 GPa have been reached. The results also disagree with the Sesame EOS but agree well with the linear-mixing model [7]. Both models are based on an approximate free energy function constructed from known theoretical limits, e.g., Sesame uses Saha and Thomas-Fermi-Dirac theories for the electronic properties and hard sphere reference systems to incorporate atoms and molecules. The double shock experiments appear to provide an independent confirmation of both the laser-driven single shock results [1] as well as some of the chemical models. Furthermore the findings were interpreted as an indication that the dissociation of molecules makes deuterium more compressible than predicted by microscopic simulations.

In this paper, we compare the Mostovych et al. [9] DS results with *ab initio* simulations from path integral Monte Carlo (PIMC) and density functional molecular dynamics (DFT-MD). We give details of the calculation of the secondary shock hugoniot curve from the simulation results. In this calculation, we use either the PIMC results or combine PIMC and DFT data. Both methods yield very similar results. We discuss whether the DS results indicate an increased compressibility for the primary hugoniot curve and therefore support the sin-

gle shock experiments, despite the different temperature and densities being reached. Furthermore, we discuss whether the process of molecular dissociation is important.

PIMC [10, 11] is a first principles simulation method that works directly with electrons and protons. Except for the problem of fermi statistics, it is an exact solution of the many-body quantum problem for a finite system in thermodynamic equilibrium. We have treated fermi statistics by restricting the paths in the region of positive density matrix by using a variational density matrix [12] consisting of a set of Gaussian single particle density matrices; a procedure that leads to lower free energy than the restrictions previously employed with free particles. The PIMC method quantitatively describes well the phenomena of electron correlation, formation of atoms and molecules, and temperature effects. The effect of fermi statistics is only important well below the fermi temperature, thus we have confidence in the results for temperatures greater than 20 000 K [4]. The PIMC results become increasingly accurate for higher temperatures.

For lower temperatures, where the effects of electronic excitations are less important, the DFT results become more reliable (relative to PIMC). We performed fixed-volume molecular dynamics simulations, employing finite-temperature DFT using the Mermin [13] functional with the electron and ion-kinetic temperatures set equal and the generalized gradient approximation [14] (GGA). Our study used the VASP plane-wave pseudopotential code, which was developed at the Technical University of Vienna [15]. This code implements the Vanderbilt ultrasoft pseudopotential scheme [16, 17], and the Perdew-Wang 91 parameterization of GGA [14].

In both shock experiments, the initial state of liquid deuterium is at a density of  $\rho_0 = 0.171 \text{ g cm}^{-3}$  at atmospheric pressure and close to zero temperature (20K). In our calculation, we match these conditions by set-

ting  $E_0 = -15.886$  eV per atom [18],  $P_0 = 0$  and using  $n_0 = \rho_0/m$  where  $m$  is the deuteron mass. If a shock wave with shock velocity  $u_s$  and particle velocity  $u_p$  is driven through the sample at state  $(E_0, n_0, P_0)$ , the new state on the other side of the shock front  $(E_1, n_1, P_1)$  follows from conservation of mass, momentum and energy [19]:

$$P_1 - P_0 = m n_0 u_s u_p, \quad (1)$$

$$\frac{n_1}{n_0} = \frac{u_s}{u_s - u_p}, \quad (2)$$

$$0 = (E_1 - E_0) + \frac{1}{2} \left( \frac{1}{n_1} - \frac{1}{n_0} \right) (P_1 + P_0) \quad (3)$$

For a given EOS,  $u_s$  and  $u_p$  can be derived from,  $u_p^2 = \xi/\eta$  and  $u_s^2 = \xi\eta$  with  $\xi = (P_1 - P_0)/n_0 m$  and  $\eta = 1 - n_0/n_1$ .

Before discussing the DS experiments, we will briefly review the comparison with results for the principle Hugoniot from laser shock wave experiments [1] with *ab initio* simulations. The Hugoniot curves from PIMC [4] and DFT-MD [5, 6] are in fairly good agreement but differ substantially from the laser-driven experimental results [1], which exhibit a significantly increased compressibility (up to  $6\rho_0$ ) compared to predictions based on empirical models such as Sesame [2]. The differences between the experimental findings and *ab initio* simulations can be characterized by the extra internal energy per particle  $E$  and pressure  $P$  needed to shift the PIMC Hugoniot curve to obtain agreement with the experimental results (see Fig. 1 in [4]). The relationship of the two shifts follows from Eq. 3:  $\delta E = \frac{1}{2}(1 - n_1/n_0) \delta pv$  where  $pv = P/n$ . The shift needed is  $\delta E = 3$  eV per atom to the internal energy or  $\delta pv = -2$  eV to the pressure. Both shifts are far outside the *ab initio* error bars (order of 0.3 eV).

In the DS experiments, a laser is used to drive a shock wave through the deuterium sample. This primary shock propagates through the sample and then reflects off an aluminum witness plate. This drives a shock wave through the aluminum plate and causes a secondary shock wave traveling in the opposite direction through the already shocked deuterium sample. We label the final DS state of the deuterium as  $(E_2, n_2, P_2)$ .

Shock waves in aluminum have been studied intensively [20] and the Hugoniot is well known. We use the linear fit formula,

$$u_s = \begin{cases} 1.339 u_p + 5.386 \text{ km s}^{-1} & \text{if } u_p < 7.557 \text{ km s}^{-1} \\ 1.1484 u_p + 6.8263 \text{ km s}^{-1} & \text{otherwise.} \end{cases} \quad (4)$$

Using the initial aluminum density of  $\rho_{Al} = 2.71 \text{ g cm}^{-3}$  and Eq. 1, we can relate the particle velocity  $u_{pAl}$  to the pressure in the shocked aluminum  $p_{Al}$ . Since the double shocked deuterium material and the shocked aluminum are in direct contact, the pressure as well as the particle velocity must be constant across the interface,  $u_{p2} = u_{pAl}$  and  $p_2 = p_{Al}$  (impedance match). We assume that the

uncertainty of the aluminum Hugoniot (Eq. 4) is approximately 1%, which corresponds to a negligible (2 GPa) error in the final shock pressure.

To study the propagation of the secondary shock front in deuterium, one preferably goes into the frame of the shocked deuterium moving with  $u_{p1}$  ( $\tilde{u}_{s2} = u_{s2} - u_{p1}$  and  $\tilde{u}_{p2} = u_{p2} - u_{p1}$ ). In this frame, Eqs. 1-3 relate the primary shock state  $(E_1, n_1, P_1)$  to the secondary shock state  $(E_2, n_2, P_2)$ .

To compare with the DS experiments [9], we need to obtain the secondary Hugoniot for a given EOS. Assuming a primary shock pressure  $P_1$ , we calculate the first shock state  $(E_1, n_1, P_1)$  and consequently  $u_{p1}$ . Then we determine the remaining variables as a function of  $P_2$  and  $u_{p2}$ . They need to satisfy two equations: the aluminum state has to be on the aluminum Hugoniot and the deuterium states 1 and 2 have to satisfy the Hugoniot relation Eq. 3. To solve the two equations for the two unknowns, we use a Newton procedure beginning with an initial guess.

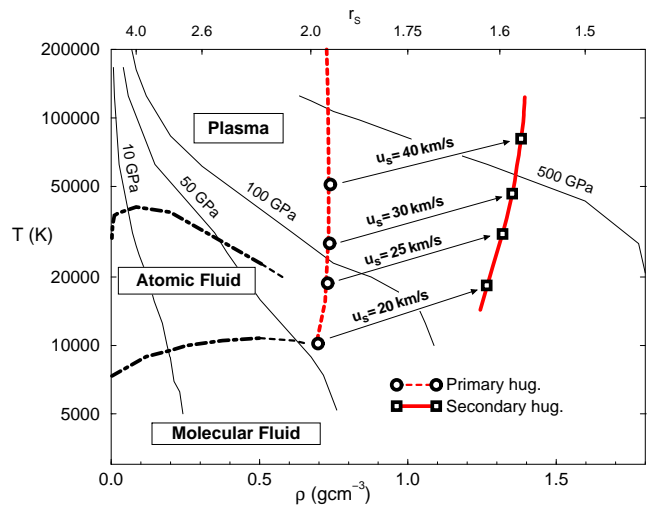


FIG. 1: Phase diagram of deuterium [11] with primary and secondary Hugoniot curves. The primary shock velocities are indicated on the arrows connecting the different shock states from Tab. I. The solid lines are isobars.

Calculating the DS Hugoniot curve in Fig. 1 requires an accurate EOS in the temperature and density range of  $10000 \leq T \leq 100000$  K and  $0.67 \leq \rho \leq 1.4 \text{ g cm}^{-3}$ . This overlaps with the region where both PIMC and DFT simulations have been applied.

Our novel EOS results calculated with PIMC and DFT simulations for the densities corresponding to  $r_s = 1.75$  and  $1.5$  are shown in Figs. 2 and 3 combined with earlier results for  $r_s = 2.0$  [4, 5]. The overall agreement of the two *ab initio* methods is quite good. The DFT results, more accurate at low temperatures, smoothly join onto the PIMC results at higher temperatures for each density. Thus we can consider combining both methods in different ways in the DS calculation (Tab. I). For high

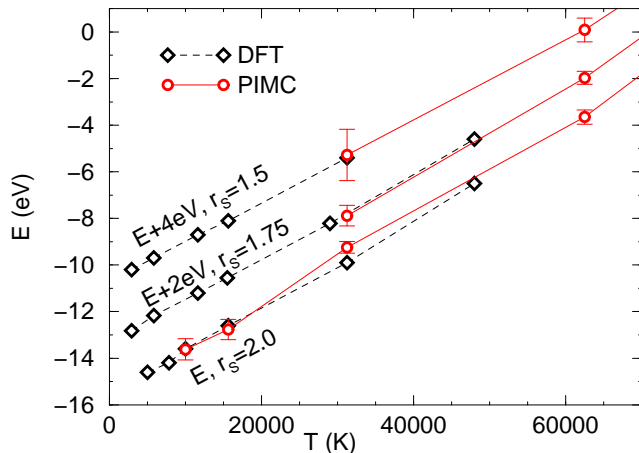


FIG. 2: Internal energy per atom vs temperature calculated with PIMC and DFT simulations. The curves for  $r_s = 1.75$  and  $1.5$  were offset by 2 and 4 eV for clarity.

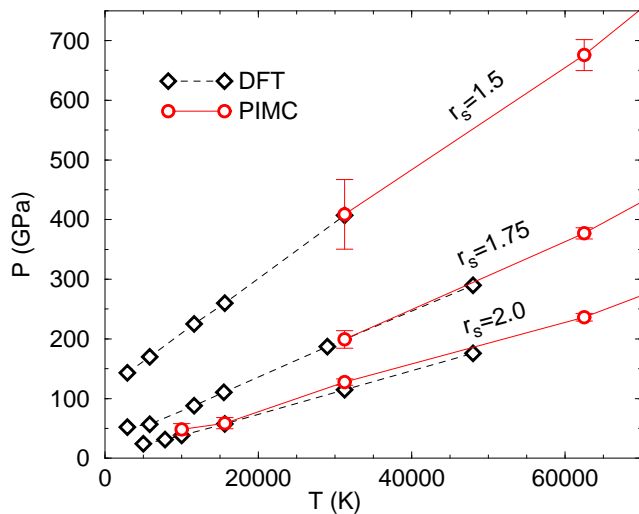


FIG. 3: Pressure vs temperature calculated with PIMC and DFT simulations.

shock velocities, we used the PIMC EOS for both shock states. This yields the most reliable secondary Hugoniot curve except for very low shock velocities such as  $u_s = 20 \text{ km s}^{-1}$ , we can also combine a primary state from PIMC with a secondary state from DFT. Alternatively, we can replace the PIMC data with the DFT EOS [5] for the first shock state.

All different ways of combining the EOS from microscopic simulations lead to very similar results compared to the DS measurements [9] as shown in Tab. I and Fig. 4. *Ab initio* methods predict a secondary shock pressure about 25% lower than measured experimentally. This is outside of the experimental error bars reported in [21] (which have increased compared to [9]). Only for  $u_{s1} = 25 \text{ km s}^{-1}$  is agreement found.

Both *ab initio* methods have statistical and finite size

TABLE I: Secondary shock pressure as a function of primary shock velocity comparing measurements with simulation results. 1 and 2 label the method used for the primary and secondary shock states. \* indicate our most reliable results and † where the DFT EOS [5] needed to be extrapolated to higher temperatures. Statistical error estimate in parentheses.

$u_{s1}$ ( $\text{km s}^{-1}$ )	Experi- ment[21] $P_2$ (GPa)	PIMC 1 PIMC 2 $P_2$ (GPa)	PIMC 1 DFT 2 $P_2$ (GPa)	DFT [5] 1 PIMC 2 $P_2$ (GPa)	DFT [5] 1 DFT 2 $P_2$ (GPa)
20		200(10)	193(6)*	231(13)	223(1)
25	400(80)	307(8)*	307(6)	327(7)	328(1)
30	590(90)	429(7)*		439(4)	
35		570(7)*		566(3)†	
40		730(5)*		709(3)†	

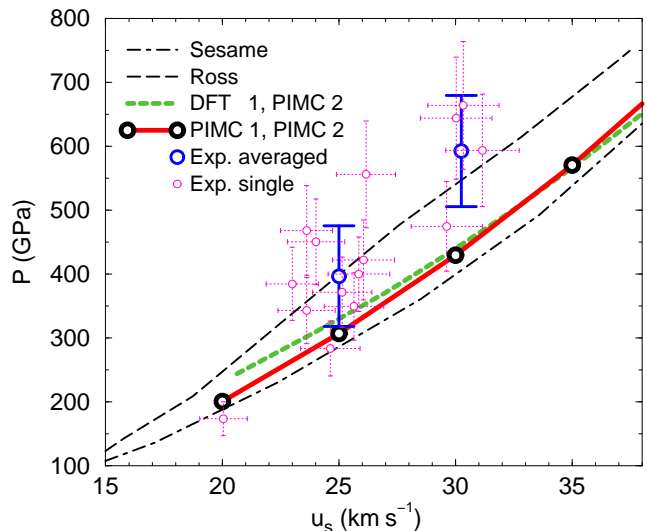


FIG. 4: Comparison of experimental and several theoretical double shock Hugoniot curves showing the secondary shock pressure as function of the primary shock velocity.

uncertainties. The statistical errors, larger for PIMC, are given in Tab. I. Finite size errors are more difficult to estimate due to the computational demand. However, very small finite-size errors, corresponding to only a 2% uncertainty of  $P_2$  were determined from other DFT simulations [6]. In addition, PIMC results [11] indicate that the finite-size dependence can not explain the difference with single shock experiments. We estimate that both types of uncertainties are significantly smaller than the deviations from the experiments.

The following analysis is based on the 15 individual shock measurements, which have been reported and shown in Fig. 4. Using a  $\chi^2$  computation leads to  $\chi^2 = 39$  for the agreement with PIMC simulations (for both first and second shocks) and  $\chi^2 = 16$  for the Ross model [7]. We note that if the experimental error bars were multiplied by 1.5 then one would obtain a reasonable agreement with the microscopic simulations. As described

for the single shock experiments, one can quantify the differences between simulation and experiments by estimating shifts  $\delta E$  and  $\delta pv$ . One finds that a shift of  $\delta E = (4.0 \pm 1.5) \text{ eV}$  or  $\delta pv = -(3 \pm 1) \text{ eV}$  needs to be applied to both shock states in order to bring the PIMC Hugoniot up in pressure to match the measurements.

We should clarify one important point. All of the approaches discussed in the present work (Sesame, PIMC, and DFT) contain dissociation within the formulation; the latter two include intermediate states and short-lived species in the dense fluid at a sophisticated quantum mechanical level. These states are part of the partition function and are therefore included in PIMC. The DFT-MD method allows one to study the dynamics of dissociation and estimate life-times [6]. Therefore, the reason for the softening of the principal Hugoniot and the behavior of the Mostovych et al. double shock experiment cannot arise primarily from the dissociation of molecular hydrogen as suggested in [9] where the comparison of different approximate free energy models had lead to this conclusion.

In conclusion, we observed significant differences when comparing our *ab initio* simulation results with the averaged DS measurements in [21]. The discrepancies are significantly larger than the combined error bars from the experiment and the simulation. As in the case of the single shock experiments, *ab initio* methods predict results which are relatively close to the Sesame model [2]. When comparing with the individual shock data points, we find agreement within the error bars only at the lower pressures. The single shock experiments [1] suggested that deuterium is significantly more compressible than predicted by *ab initio* simulations. A substantial increase in internal energy or decrease in pressure would be necessary to bring the *ab initio* EOS in agreement with these measurements. We find that comparable shifts in energy or pressure are required to reach agreement between the DS experiments [9] and microscopic simulation results. Therefore, it can be concluded that both types of laser-driven experiments are in relative agreement with each other and disagree with *ab initio* methods. Clearly, more theoretical and experimental work is necessary to resolve the discussed discrepancy.

Work performed under the auspices of the U.S. Depart-

ment of Energy though the University of California at the Lawrence Livermore National Laboratory (W-7405-Eng-48, CSAR subcontract B341494) and at the Los Alamos National Laboratory (W-7405-Eng-36). We acknowledge useful discussions with Dr. M. Knudson.

- 
- [1] I. B. Da Silva *et al.*, Phys. Rev. Lett. **78**, 783 (1997); G. W. Collins *et al.*, Science **281**, 1178 (1998).
  - [2] G. I. Kerley, in *Molecular Based Study of Fluids*, edited by J. M. Hail and G. A. Mansoori (ACS, Washington DC, 1983), p. 107.
  - [3] M.D. Knudson *et al.*, Phys. Rev. Lett. (in press).
  - [4] B. Militzer and D. M. Ceperley, Phys. Rev. Lett. **85**, 1890 (2000).
  - [5] T. Lenosky *et al.*, Phys. Rev. B **61**, 1 (2000); L. Collins *et al.*, Phys. Rev. **63**, 184110 (2001).
  - [6] G. Galli *et al.*, Phys. Rev. B **61**, 909 (2000); S. Bagnier *et al.*, Phys. Rev. E **6302**, 5301 (2001).
  - [7] M. Ross, Phys. Rev. B **58**, 669 (1998).
  - [8] D. Saumon and G. Chabrier, Phys. Rev. A **46**, 2084 (1992).
  - [9] A. N. Mostovych *et al.*, Phys. Rev. Lett. **85**, 3870 (2000).
  - [10] D. M. Ceperley, Rev. Mod. Phys. **67**, 279 (1995); D. M. Ceperley, J. Stat. Phys. **63**, 1237 (1991).
  - [11] B. Militzer and D. M. Ceperley, Phys. Rev. E **63**, 066404 (2001).
  - [12] B. Militzer and E. L. Pollock, Phys. Rev. E **61**, 3470 (2000).
  - [13] N.D. Mermin, Phys. Rev. **137A** (1965) 1441.
  - [14] J. P. Perdew, in *Electronic Structure of Solids*, ed. by F. Ziesche and H. Eschrig (Akademie Verlag, Berlin, 1991).
  - [15] G. Kresse and J. Hafner, Phys. Rev. B **47**, RC558 (1993); G. Kresse and J. Furthmüller, Comput. Mat. Sci. **6**, 15–50 (1996); G. Kresse and J. Furthmüller, Phys. Rev. B **54**, 11169 (1996).
  - [16] D. Vanderbilt, Phys. Rev. B **41** 7892 (1990).
  - [17] G. Kresse and J. Hafner, J. Phys. Condens. Matter **6**, 8245 (1994).
  - [18] W. Kolos and L. Wolniewicz, J. Chem. Phys. **41**, 3674 (1964).
  - [19] Y. B. Zeldovich and Y. P. Raizer, *Physics of Shock Waves and High-Temperature Hydrodynamic Phenomena* (Academic Press, New York, 1966).
  - [20] A. Mitchell and W. Nellis, J. Appl. Phys. **52**, 3363 (1981)
  - [21] A. Mostovych *et al.*, Phys. Plasmas **8**, 2281 (2001).